SUPPORTING INFORMATION

Direct electrochemistry of *Shewanella oneidensis* cytochrome *c* nitrite reductase: evidence for interactions across the dimeric interface

Evan T. Judd,[1,2] Matthew Youngblut,[3] A. Andrew Pacheco,[3] Sean J. Elliott[1,2]*

Author Addresses

1. Department of Chemistry, Boston University, 590 Commonwealth Avenue, Boston, MA 02215

2. Molecular Biology, Cell Biology, and Biochemistry Program, Boston University, 5 Cummington St. Boston MA 02215

3. Department of Chemistry and Biochemistry, University of Wisconsin-Milwaukee, Milwaukee, WI 53211.

*** Corresponding Author Information:**

Sean J. Elliott, Department of Chemistry, 590 Commonwealth Ave. Boston, MA 02215, tel 617-653-4484, fax 617-353-6466, email: elliott@bu.edu

SUPPLEMENTARY METHODS

Modeling of soNrfA catalytic voltammograms. The reductive half of cyclic voltammograms of soNrfA nitrite and hydroxylamine turnover were baseline subtracted to remove the background contribution to the catalytic waves due to electrode charging using the SOAS package (Fourmond et al. 2009. Bioelectrochemistry 76, 141-147). All subsequent analysis was also done using SOAS. Reductive waves produced in the presence of 15 μM nitrite were fit to two models: Model A and Model B. Model A accounts a catalytic wave consisting of two separate components, such that both the onset of catalysis (component 1, E_{cat}) and E_{sw} (component 2) are due to one-electron processes (Figure S2, A). Model B also accounts for a catalytic wave consisting of two separate components, except the onset of catalysis (component 1, E_{cat}) is due to a two electron process and E_{sw} (component 2) is due to a one-electron process. The resulting best fits are plotted with the data in Figure S2, panel A.

Baseline subtracted reductive waves produced in the presence of 1.9 mM nitrite and 1.2 mM hydroxylamine were each fit to two models: Model A and Model C. Model A, as described above, is composed of two one-electron components (E_{cat1} and E_{cat2}). Model C assumes catalytic waves are composed of two components and both of the onset of catalysis (component 1, E_{cat1}) and the lower potential catalytic feature (component 2, E_{cat2}) are due to two-electron features. The resulting best fits are plotted with data in Figure S2, Panels A and B.

SUPPLEMENTARY FIGURES

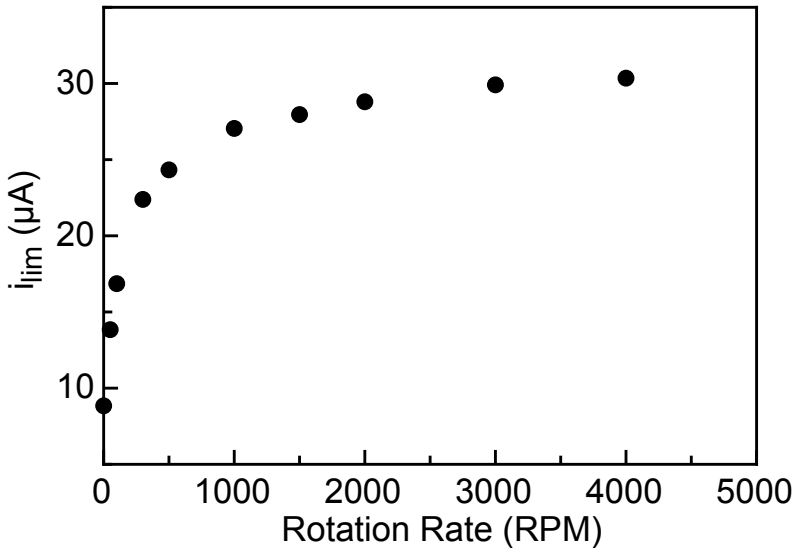

Supplementary Figure 1. Dependence of limiting current on electrode rotation rate. Scans recorded at 487 μM nitrite, pH 7, 2 mM $CaCl_2$, 20°C. Limiting current measured at -550 mV. At 3000 rpm magnitude of limiting current is essentially independent of rotation rate.

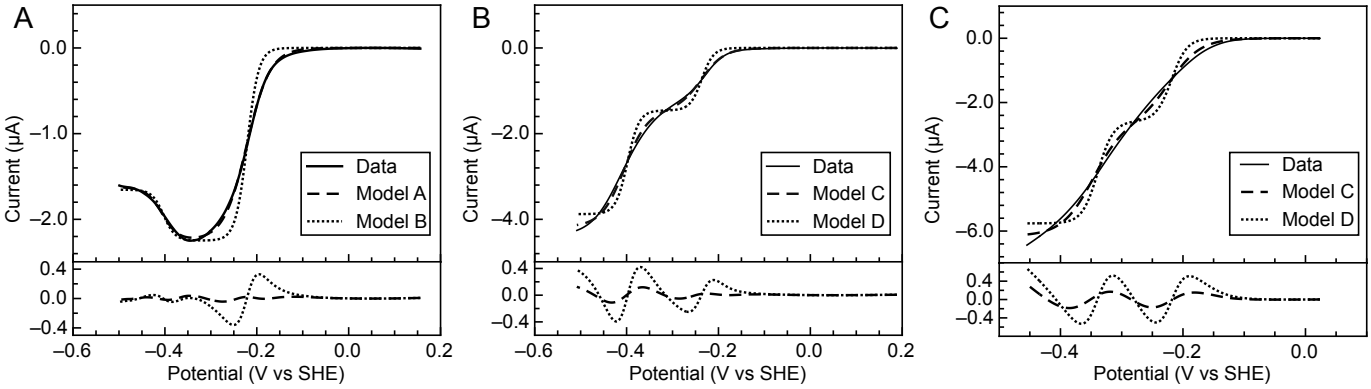

Supplementary Figure 2. Baseline-subtracted reductive scans of catalytic voltammograms for nitrite (A,B) and hydroxylamine (C) turnover. All scans were recorded at pH 8.3, 20°C, 20 mV/s, 2 mM $CaCl_2$, 3000 rpm electrode rotation rate. Data is fit to different models discussed in supplementary methods. Residuals of each fit are shown in the subplots. (A) soNrfA catalysis at 15 μM nitrite. (B) soNrfA catalysis at 1.9 mM nitrite. (C). soNrfA catalysis at 1.2 mM hydroxylamine.

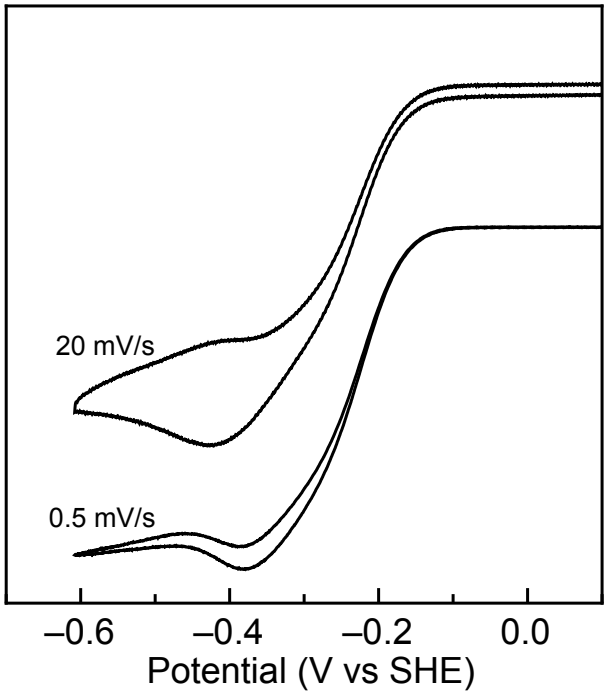

Supplementary Figure 3. Superimposability of oxidative and reductive waves during nitrite turnover depends on scan rate. Scans recorded at 500 μM nitrite, pH 7, 2 mM $CaCl_2$, 20°C, 3000 rpm.

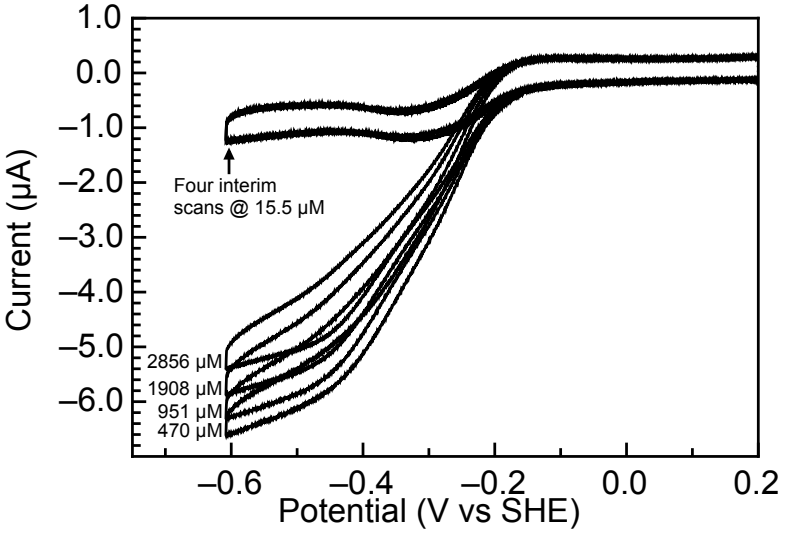

Supplementary Figure 4. Film loss can not account for decrease in limiting current at high nitrite concentrations. Experiment was carried out at pH 8.3, 2 mM $CaCl_2$, 18°C, 3000 rpm. Four scans showing decrease in i_{lim} with increasing nitrite concentrations. After each scan at high nitrite concentrations, the working electrode was transferred to an electrochemical cell containing 15 μM nitrite. This was repeated between each of the scans at high nitrite concentrations. There were no differences in i_{lim} between these four interim scans. Thus, the decrease in ilim at higher concentrations is not due to film loss.

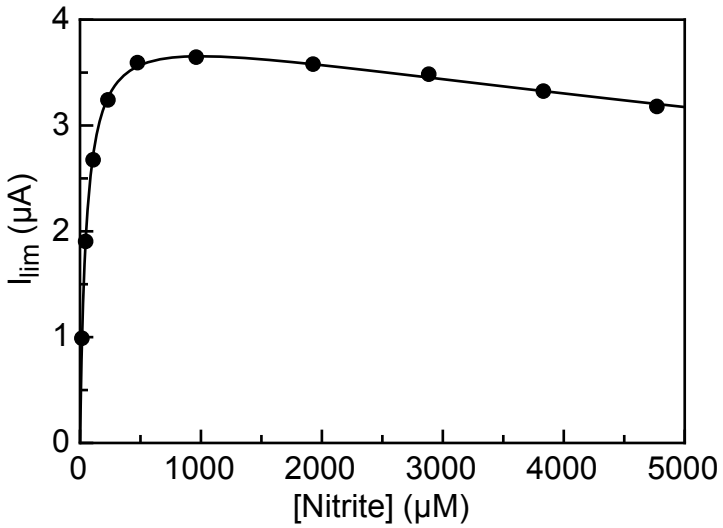

Supplementary Figure 5. Variation in limiting current as a function of nitrite concentration in the buffer containing 150 mM NaCl. Experiments carried out at pH 8.3, 20°C, 20 mV/s, with an electrode rotation rate of 3000 rpm. Limiting current was measured at -550 mV. Kinetic values, determined by fitting to equation 1, were K_m = 47 ± 10 μM, V_{max} 4.2 ± 0.3 μA, K_I 16 ± 6 mM. These values are consistent with those determined in buffer containing 100 mM NaCl.

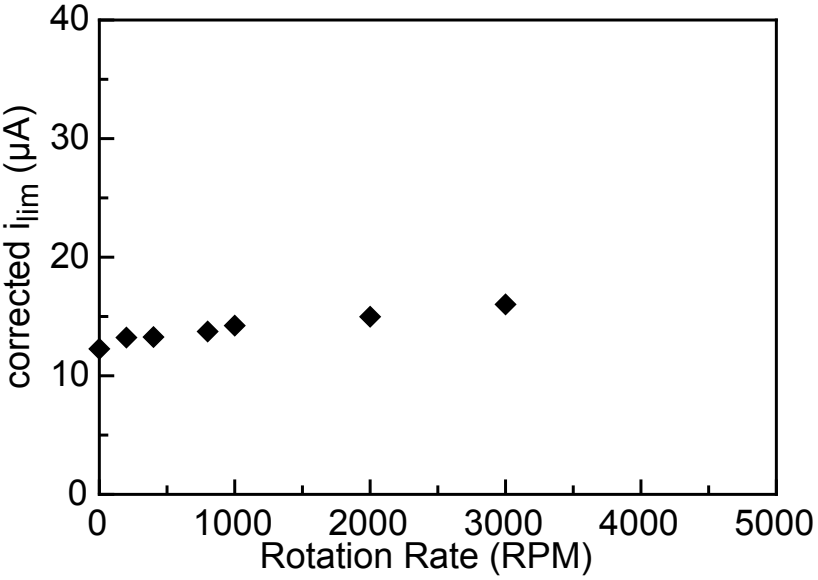

Supplementary Figure 6. Rotation rate dependence of limiting current for hydroxylamine turnover. Experiment carried out at 24 mM hydroxylamine, pH 8.3, 20 mV/s. Limiting currents are corrected for film loss. Plot is on the same scale as nitrite turnover rotation rate dependence for comparison. While there is a slight increase in magnitude of i_{lim} with rotation rate, the increase is similar to that observed for nitrite turnover. At this rotation rate, we take this data to mean that substrate diffusion at the electrode only makes up a small component of i_{lim}.

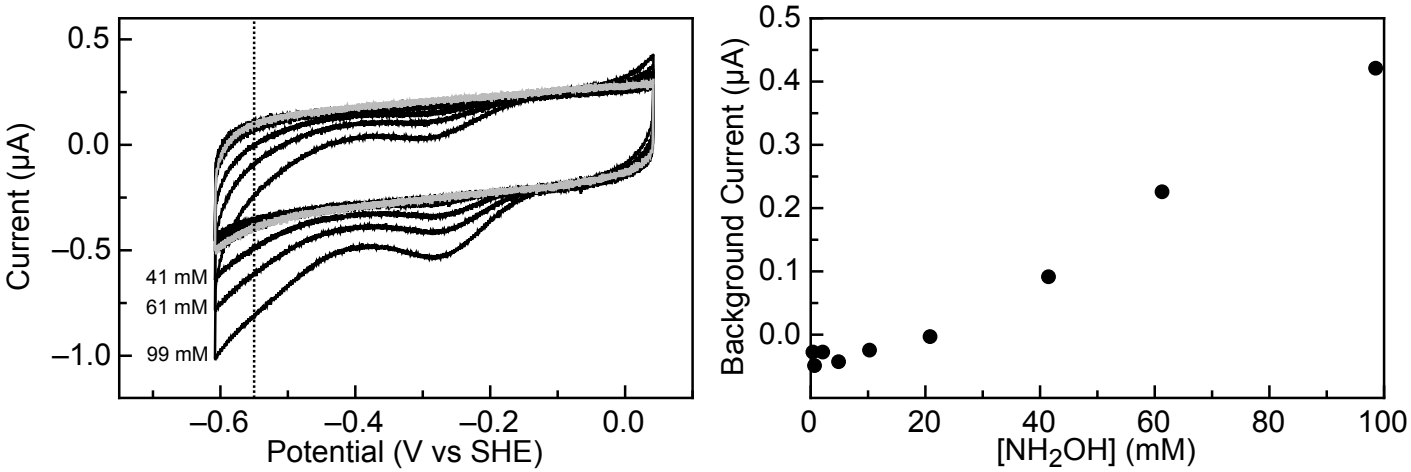

Supplementary Figure 7. Reactivity of hydroxylamine with PGE electrodes. Experiments were carried out at 20°C, 3000 rpm rotation rate, pH 8.3, 20 mV/s, 2 mM $CaCl_2$. Dotted vertical shows -550 mV. (A) Plot of voltammograms for bare electrodes in buffer containing different concentrations of hydroxylamine. Red trace shows electrochemical response for a bare PGE electrode in hydroxylamine free buffer. Traces for the three hydroxylamine concentrations that showed observable current at -550 mV are labeled. All other traces are unlabeled and nearly identical to baseline. (B) Magnitude of reductive current normalized to baseline scan at -550 mV for each hydroxylamine concentration. Contribution is essentially zero until hydroxylamine concentration is greater than 20 mM.